Activated porous carbon wrapped sulfur sub-microparticles as cathode materials for lithium sulfur batteries

Y Wang[1], Y L Yan[1,*], B Ren[1], R Yang[2], W Zhang[1] and Y H Xu[1]

[1] School of Materials Science and Engineering, Xi'an 710048, China
[2] School of Science, Xi'an University of Technology, Xi'an 710048, China

E-mail: *yyl3550@xaut.edu.cn

Abstract. The lithium-sulfur batteries holds a high theoretical capacity and specific energy, which is 4-5 times larger than that of today's lithium-ion batteries, yet the low sulfur loading and large particles in the cathode greatly offset its advantage in high energy density. In the present paper, a liquid phase deposition method was introduced to synthesize sub-micro sulfur particles, which utilized as cathode materials after composed with activated porous carbon. Compared with common sublimed sulfur cathodes, as-obtained composite cathode shows an enhanced initial discharge capacity from 840.7 mAh/g to 1093 mAh/g at C/10. The reversible specific capacity after 50 cycles increased from 383 mAh/g to 504 mAh/g. The developed method has the advantages of simple process, convenient operation and low cost, and is suitable for the industrial preparation of lithium/sulfur batteries.

Keywords: lithium sulfur batteries, liquid phase deposition, sub-micro sulfur particles, porous carbon

1. Introduction

With the rapid development of electric vehicles and mobile electronic devices, there is an urgent need to develop higher energy density batteries. The largest theoretical specific capacity of conventional lithium ion battery cathode material was only 300mAh/g [1], however, the actual specific capacity is lower than 300 mAh/g. It has become increasingly difficult to meet the development of the market demand for the high capacity secondary batteries. The theoretical specific capacity and specific energy of lithium sulfur secondary batteries are up to 1675 mAh/g and 2600 Wh/kg [2,3], respectively. Besides, the cathode active material of element sulfur is very abundant in nature, low cost and environmental friendly [4]. It shows good performance and bright future in application, which is the research topic in the field of chemical power source.

However, in spite of these advantages, the practical application of Li-S batteries is still facing with several problems, including the stability of lithium metal and the insulating nature of pure sulfur with extraordinary low conductivity of $5\times10\text{-}30$ $S\cdot cm^{-1}$ [5] at room temperature. It is difficult to have sufficient electrochemical contact between the cathode active materials of sulfur, conductive carbon and the current collector, thus resulting in the insufficient utilization of sulfur [6,7]. Various attempts to overcome the above-mentioned problems appeared, most of which focus on enhancing the electrical conductivity of the cathode and trapping the polysulfides in a conducting matrix during cycling. Conducting matrix includes porous carbon [8,9], graphene [10,11], carbon nanotubes [12,13], metal oxides [14,15], and conductive polymers [16,17]. In addition, it can start from the size of the elemental sulfur. However, at present, the particle size of sulfur usually distributes in micron level, such as

sublimed sulfur. If sublimed sulfur is use directly to be the cathode in lithium batteries, it is not benefit to develop the potential performance of battery. It is found that the construction of cathode material with micro/nano structure is an effective way to improve the electrochemical performance of lithium sulfur battery, sub-micro sulfur [18] has the advantages of small size, large specific surface area, rich pore volume, which can improve the electrochemical performance of the battery, so it is more suitable for application in lithium/sulfur batteries.

At present, the preparation of micro/nano sulfur materials mainly are used by high temperature gas phase solidification method, which needs to be carried out under high temperature and inert gas protection. It is not suitable for industrial production due to its harsh preparation conditions, high energy consumption and high cost. Guo [19] prepared nano sulfur material with regular spherical structure by water-oil two phase micro emulsion method. However, this method required a large amount of organic solvent and surfactant, and the subsequent cleaning process was more complicated. Recently, liquid phase deposition method [20,21] was used to prepare micro/nano materials efficiently, which was the moderate chemical reaction in the solution. Compared with the preparation method above, it is easier to control the chemical reaction process of liquid phase deposition method with the simple process and low cost. For example, Shin [22] used liquid phase deposition method to synthesize colloidal micron sulfur.

Herein, in this paper, we prepared sub-micro sulfur/activated porous carbon (AC) composites by a simple method as the cathode material in lithium sulfur batteries. Using sub-micro S prepared by the liquid phase deposition as an active material. AC was used as a conductive matrix with excellent chemical adsorption capacity of lithium sulfides and polysulfide, which enhanced electrochemical performances remarkably. Because of the smaller particle size of sub-micro S, it is more uniformly distributed in activated carbon matrix. Compared with sublimed S, the use of smaller scale sub-micro S indirectly enhance the conductivity of the active material, and greatly improves the charge and discharge specific capacity of lithium sulfur batteries. In addition, adsorption effect of activated carbon for smaller sub-micro S particles is stronger, and the distribution of sulfur particle is expanding in the activated carbon. It will significantly reduce the shuttle effect [23-25] and control polysulfide dissolved into the electrolyte during cycle process, thus improving sulfur utilization and cycle stability.

2. Experimental

2.1. Synthesis of sub-micro sulfur

The synthesis of sub-micro S by liquid phase deposition. In a typical reaction, first, sodium thiosulfate pentahydrate ($Na_2S_2O_3 \cdot 5H_2O$, analytical grade, 7.75 g) was dissolved in deionized water (a laboratory made, 78 mL) with magnetic stirring (0.4M of $Na_2S_2O_3 \cdot 5H_2O$) at the ice bath (0-5 ℃), named solution A. Secondly, PEG-400(5 ml) was added into 10 mL hydrochloric acid (HCl, 1 M), named solution B. Third, solution B was added dropwise (60 drops/min) into solution A. In order to react completely, the reaction process remained for 2 h at room temperature with magnetic stirring and ultrasonic treatment, after which the product was filtered and washed several times with deionized water until the value of pH was reached 7. Finally, the yellow suspension was collected and dried in an air-oven at 55 ℃ for 24 h. Sub-micro S powers were obtained. The reaction equation in the liquid phase occurred as equation (1).

$$Na_2S_2O_3 \cdot 5H_2O + 2HCl \rightarrow S\downarrow + SO_2\uparrow + 2NaCl + 6H_2O \quad (1)$$

2.2. Synthesis of sulfur/activated carbon composites

Sub-micro S or sublimed S (analytical grade)/activated carbon (AC, Shaanxi XinHua Carbon Industry) composites were prepared via melt infusion. Typically, sulfur powders and AC were taken in a 6:4 weight ratio and mixed well. The mixture was then transferred into a sealed stainless steel vessel (50 ml) and placed in an oven heated at 155 ℃ for 8 h to obtain the S/C composites.

2.3. Materials characterization

To evaluate the characteristic of the S, S/AC composite, X-ray diffraction (Shimadzu XRD-7000, with Cu Ka radiation, λ=1.5406 Å) was conducted to investigate the compositions of the as-prepared product. The morphology and energy dispersive spectroscopy (EDS) mapping of samples were obtained with JEOL JSM-6610 scanning electron microscopy (SEM) and JEOL 3100 transmission electron microscope (TEM), respectively. The particle size of sulfur was test by laser particle analyzer (LPA, BT-2003).

2.4. Electrochemical testing

The cathode was prepared by making a slurry of the S/C composite, KS-6 conductive graphite, and polyvinyledene fluoride (PVDF) binder in a weight ratio of 80:10:10, using N-methyl-2- pyrrolidone (NMP) as the solvent. The slurry was then cast onto an aluminum foil using a glass rod to make ~20 micron thick films followed by drying at 50 ℃ in an oven for 12 h. Lithium metal was used as the anode. A microporous polypropylene Celgard 2300 membrane was used as the separator. 1 M Lithium Bis (Trifluoromethanesulfonyl) Imide (LiTFSi) and 1wt% lithium nitrate ($LiNO_3$) dissolved in a mixture of 1, 3-Dioxolane (DOL) and Dimethoxyethane (DME) (1:1 by volume) was used as the electrolyte. CR2025 type coin cells were assembled in a glove box under inert argon atmosphere. Galvanostatic charge and discharge tests were carried out using a Neware battery tester in the voltage range of 1.5-3.0 V (vs Li^+/Li).

3. Results and discussion

XRD patterns (figure 1) were recorded to investigate the state of the synthesized sub-micro S and AC in the S/C materials. Firstly, pure sulfur displays sharp diffraction peaks that agree well with the characteristic pattern of S8 which matches with the standard value (JCPDF NO. 08-0247), while carbon materials only show two broad diffraction peaks at ~ 24° and ~43°, indicating amorphous characteristics. Furthermore, compared with the pure sub-micro S sample, the sub-micro S/AC composites shows the weaker diffraction peaks than that of bulk crystalline sulfur, indicating that there is some sulfur distributed on the surface of the activated carbon, and the other sulfur exists as highly dispersed fine particles in the pores of carbon matrix. It may alleviate the insulation issue of sulfur, and is good for electron transport in the electrode to be fabricated.

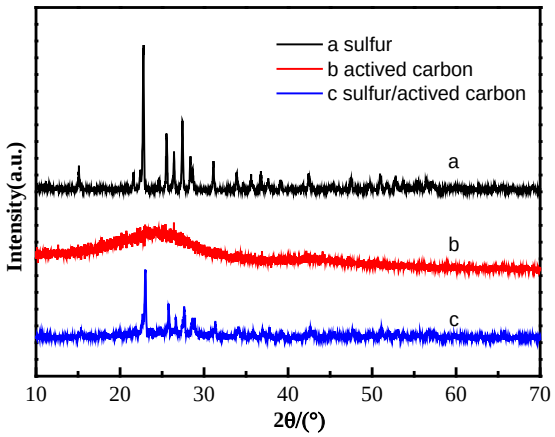

Figure 1. XRD patterns of sub-micro S, AC, sub-micro S/AC.

Figure 2(a) is the SEM image of sub-micro sulfur precipitated in aqueous solution. The particle size of as-prepared sulfur particles is below 1 μm uniformly, and agglomeration phenomenon appear slightly. According to the TEM image of sulfur particles (figure 2(b)), the size of larger particles is about 250 nm. Moreover, some smaller sulfur particles below 100 nm are also presented at the upper right corner in figure 2(b).

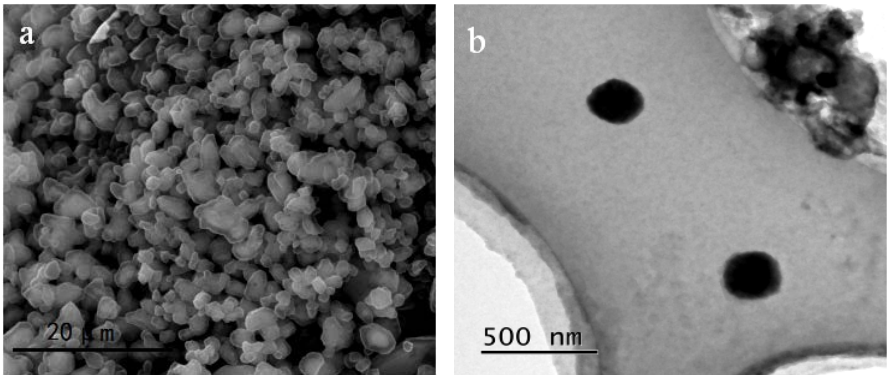

Figure 2. (a) SEM images ,and (b) TEM images of the sub-micro S.

In order to precisely determine the distribution of particle size of sulfur, the sample was tested by laser particle size analyzer and the test result in exhibited in figure 3. As can be seen, the size of the sulfur particles mainly distributes in 150nm±10 nm, and the minority of sulfur particles' size is distributed in 100nm±10 nm, which confirms the particle size of sulfur is at the sub-micro level. The size control of sub-micro sulfur particles attributes into several reasons, such as (1) the effect of surfactant (PEG) in B solution, (2) slow adding rate of B into A, and (3) the inhibited growing rate caused by ice bathing. As a result, the particle size of sulfur can be reduced to sub-micro, even close to the nano scale.

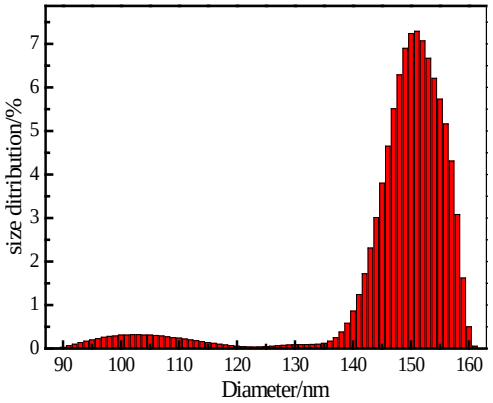

Figure 3. The laser particle-size distribution of sub-micro S.

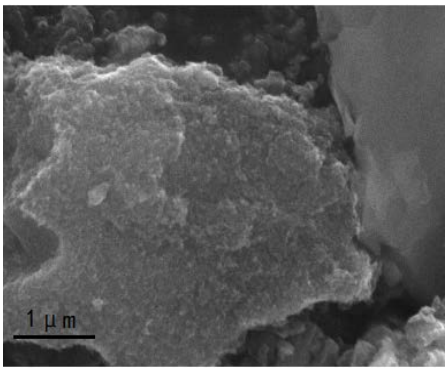

Figure 4. SEM image of AC.

Figure 4 is the SEM image of AC particles. It shows that the AC particles possess a irregular shape and uneven surface. It also has a large number of pores, generally for mesoporous scale (2-50 nm) [26].

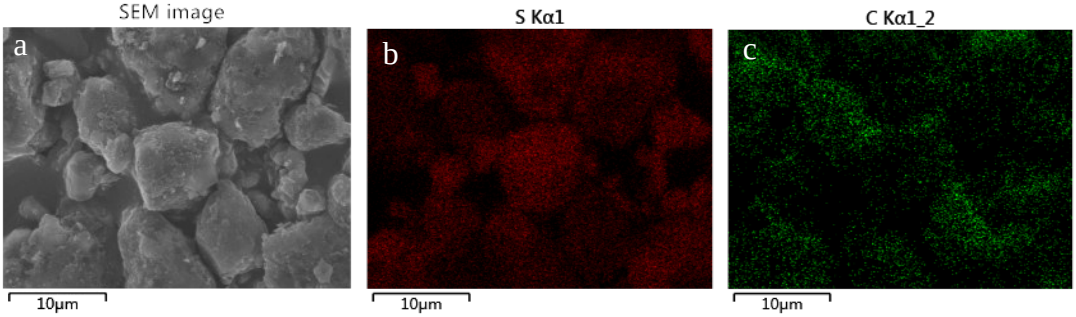

Figure 5. SEM images of (a) the sub-micro S/AC composite, (b) EDS sulfur and (c) EDS carbon mapping of the region shown in (a).

The SEM image and EDS analysis of sub-micro S/AC composite is shown in figure 5. After sub-micro S and AC was compounded, the number of surface pores decreased significantly(figure 5(a)). It suggests that part of sulfur particles have been filled into the pores of AC. It is consistent with the decreasing of diffraction intensity of sulfur element in the XRD result of the previous figure 1. The distributions of S and C elements are shown in figure 5(b) and 5(c), respectively. As can be seen that the majority of sulfur particles distribute uniformly in carbon matrix.

The sub-micro S/AC composites and the sublimed S/AC composites were both assembled into Li/S battery as cathode materials and the charge and discharge performances were tested at 0.1 C. The testing results are shown in figure 6. The discharge platforms are at the vicinity of 2.3 and 2.1 V, and the former corresponds to elemental sulfur is oxidized to sulfur compounds (Li_2S_n, $n \geqslant 4$) process, while the later corresponds to the high valence sulfides (Li_2S_n, $n = 4$) reduced to low valence sulfides (Li_2S_n, $n < 4$) and the Li_2S process. The first discharge capacity of sub micron S/AC battery is up to 1097 mAh/g, higher than that of the sublimed S/AC battery which is only 870 mAh/g. It shows that the prepared sub-micron S can promote the sulfur capacity in battery. Due to the smaller size of sub micron S, shortening the ion diffusion paths in the transmission and promoting the transfer of charge at the same time.

The corresponding cycle properties of sub micron S/AC battery and sublimed S/AC battery at 0.1C for 50 times are also shown in figure 6(b). It can be seen that the sub-micro S/AC composite assembled battery in the first 15 cycles, the capacity decay rapidly, which is mainly caused by internal complex irreversible electrochemical reaction in the battery [27]. Since the sixteenth cycle, the discharge specific capacity tends to be stable. After 50 cycles, it can still maintain the capacity of 503.7 mAh/g, about 46.1% of the initial capacity. At the same time, the charge and discharge efficiency is almost up to 100%. However, the specific capacity of sublimed S/AC battery decreases quickly in the previous 4 cycles. After 50 cycles, it can still maintain the initial capacity of about 44% (382.9 mAh/g), and the charge and discharge efficiency is about 98.8%. In summary, the discharge specific capacity and capacity retention rate of sub-micro S/AC composites battery is better than that of sublimed S/AC composites.

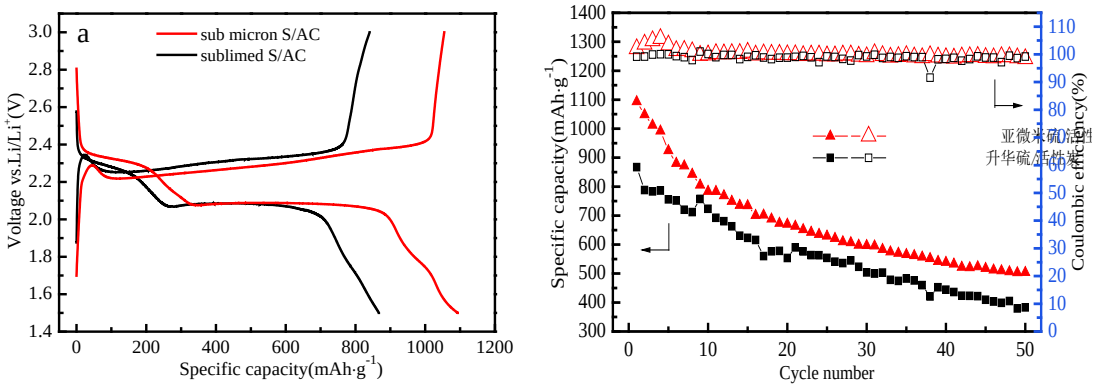

Figure 6. Electrochemical performance of sub-micro S/AC and sublimed S/AC composites. (a) Charge/discharge voltage profiles of electrodes at 0.1C between 1.5 and 3 V, (b) Comparison of the cycling performance over 50 cycles at 0.1C.

The EIS measurements were performed on coin cells with the same loading of the sulfur and the results are shown in figure 7. The resistance ($R_Ω$), corresponding to the intercept at the real axis, is determined by the ionic resistance of the electrolyte, the intrinsic resistance of the active materials, and the contact resistance at the active material/current collector interface. The charge transfer resistance (R_{ct}), corresponding to the semicircle in the high-frequency region, represents the kinetic resistance of the electrochemical reaction at the electrode-electrolyte boundary. The Warburg impedance, corresponding to the inclined line at low frequency, is associated with Li-ion diffusion in the electrode [28, 29].

Before cycling, both the EIS results from sub micron S/AC battery and sublimed S/AC battery exhibit typical semicircles at high frequencies and short inclined lines in the low frequency region as shown in figure 7(a). The R_{ct} is 221 Ω for sub-micro S, which is lower than that for sublimed sulfur (330 Ω). As all known, the R_{ct} is significantly affected by the area of interface for the electrochemical reaction, as well as the transfer rate of Li^+, and the conductivity of electrons. In the sub micron S/AC composites, as the reduction of sulfur particle size, the attachment sites between the sulfur particles and the pore walls of AC matrix are increased. Thereby the reaction active sites between cations, anions and electrolyte during the charging and discharging process are improved. Thus, larger reaction zones and better electron transfer rate result a smaller R_{ct}. Moreover, the Li-ion diffusion rate of sub micron S/AC composites cathode materials is as shown in the Nyquist plots in the low- frequency region.

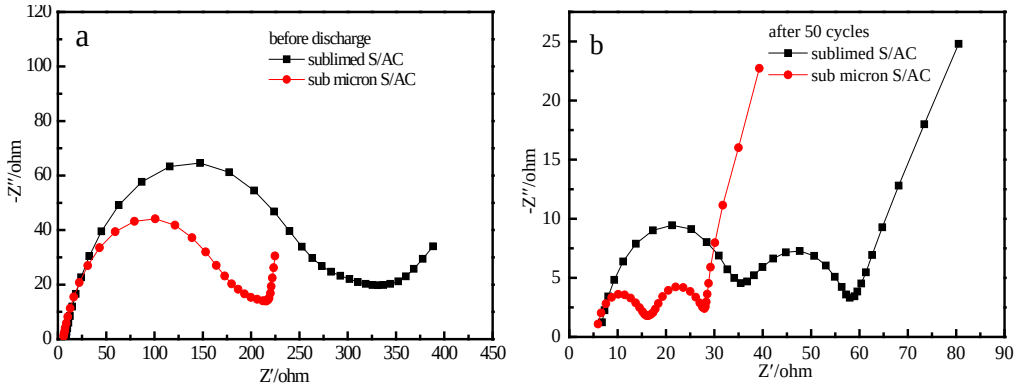

Figure 7. Electrochemical impedance response of Li/S batteries.
(a) before discharge, and (b) after 50 cycles.

After 50 cycles (figure 7(b)), there are two different semicircles followed by a sloping line in the EIS. Generally, the high-frequency semicircle attributes to from the inter-facial charge transfer process, and the semicircle in the medium frequency range is related to the solid-electrolyte-interface (SEI) film resistance caused by the formation of Li_2S or Li_2S_2 on the surface of cathode, and the straight line is ascribed to the diffusion of Li ions in the matrix. As can be seen, both the resistance (R_{ct}) and Li-ion diffusion rate of sub micron S/AC battery are still better than that of sublimed S/AC battery after 50 cycles. The R_{ct} after cycling are decreased remarkably in comparison with that before cycling (from 221 Ω to 28 Ω for sub micron S/AC battery and from 330 Ω to 58 Ω for sublimed S/AC battery), which may be due to the infiltration of the electrolyte and chemical activation process for the dissolution and redistribution of the active materials [30].

4. Conclusions

In summary, a sub-micro S particles, particle size distributed in 150nm±10nm, was successfully fabricated through the liquid phase deposition method. Then it was used to prepare a sub-micro S/AC composite by ball-milling and melt diffusion process. The sulfur element dispersed uniformly in AC matrix from the EDS map. The the sub-micro S/AC cell presented higher initial discharge capacity 1097 mAh/g at 0.1 C and better cycle performance after 50 cycles than the sublimed S/AC cell. This is due to the smaller resistance and faster Li^+ transfer rate in the sub-micro S/AC cell, which is verified by EIS testing. Consequently, the smaller particle size of sulfur played a important role in enhancing the electrochemical performance of sub-micro S/AC composite cathode. The reaction active sites between the positive ions, negative ions and the electrolyte were improved significantly. It is believed that reducing the sulfur particle size is good for high performance Li-S batteries applications.

Acknowledgment

The authors thank the the International Science and Technology Cooperation Program of China (Nos. 2015DFR50350) and Scientific Research Program Funded by Shaanxi Provincial Education Department (Nos. 15JK1536, 14JS047) for the financial support through a laboratory-directed research and development. The synthesis and structural characterization of the bimodal porous materials and the S/C composites were conducted at Xi'an University of technology (Innovation project, Nos. 2015CX002, 2014CX024).

References

[1] Nagata H and Chikusa Y 2014 *J. Power Sources* **264** 206–210
[2] Bruce P G, Freunberger S A, Hardwick L J and Tarascon J M 2012 *Nat. Mater.* **11** 19–29
[3] Wang W, Yu Z B, Yuan K G, Wang A and Yang 2011 *Prog. Chem.* **23**(2/3) 540–546
[4] Goodenough J B and Kim Y 2010 *Chem. Mater.* **22** 587–603
[5] Tarascon J M and Armand M 2001 *Nat.* **414** 359–367
[6] Ji X and Nazar L F 2010 *J. Mater. Chem.* **20** 9821–9826
[7] Cheon S E, Ko K S, Cho J H, Kim S W, Chin E Y and Kim H T 2003 *J. Electrochem. Soc.* **150** A796–A799
[8] Qu Y, Zhang Z, Zhang X, Ren G D, Wang X W, Lai Y Q, Liu Y X and Li J 2014 *Electrochim. Acta* **137** 439–446
[9] Liang C, Dudney N J and Howe J Y 2009 *Chem. Mater.* **21** 4724–4730
[10] Wang H, Yang Y, Liang Y, Robinson J T, Li Y, Jackson A, Cui Y and Dai H 2011 *Nano Lett.* **11** 2644–2647
[11] Jiang Y, Lu M N, Ling X T, Jiao Z, Chen L L, Chen L, Hu P F and Zhao B 2015 *J. Alloys Compd.* **645** 509–516
[12] Guo J, Xu Y and Wang C 2011 *Nano Lett.* **11** 4288–4294
[13] Dörfler S, Hagen M, Althues H, Tübke J, Kaskel S and Hoffmann M J 2012 *Chem. Commun.* **48** 4097–4099
[14] Wei S Z, Li W, Cha J J, Zheng G, Yang Y, McDowell M T, Hsu P C and Cui Y 2013 *Nat. Commun.* **4** 1331
[15] Zhang Y, Bakenov Z, Zhao Y, Konarov A, The Nam Long Doan, Sun K E K, Yermukhambetova A and Chen P 2013 *Powder Technol.* **235** 248–255
[16] Xiao L, Cao Y, Xiao J, Schwenzer B, Engelhard M H, Saraf L V, Nie Z, Exarhos G J and Liu J 2012 *Adv. Mater.* **24** 1176–1181
[17] Li G C, Li G R, Ye S H and Gao X P 2012 *Adv. Energy Mater.* **2** 1238–1245
[18] Chen J J, Jia X, She Q J, Wang C and Zhang Q 2010 *Electrochimi. Acta* **55** 8062 – 8066
[19] Guo Y, Zhao J, Yang S, Yu K and Wang Z 2006 *Powder Technol.* **162** 83–86
[20] Ni H and Fan L Z 2012 *J. Power Sources* **214** 195–199
[21] Guo W L and Wang X K 2004 *Technol. Dev. Chem. Ind.* **33** 1−3
[22] Shin J H and Cairns E J 2008 *J. Electrochem. Soc.* **155** A368–A373
[23] Diao Y, Xie K, Xiong S and Hong X 2013 *J. Power Sources* **235** 181–186
[24] Elezari R, Salitra G, Garsuch A, Panchenko A and Aurbach D 2011 *Adv. Mater.* **23** 5641–5644
[25] Wang Q, Jin J, Wu X, Ma G and Yang J 2014 *Phys. Chem. Chem. Phys.* **16** 21225–1229
[26] Yang C S, Yun S J and Jeong H K 2014 *Curr. Appl. Phys.* **14** 1616–1620
[27] Diao Y, Xie K, Hong X B and Xiong S Z 2013 *Acta Chim. Sinica* **71** 508–518
[28] Deng Z F, Zhang Z A, Lai Y Q, Liu J, Li J and Liu Y X 2013 *J Electrochem. Soc.* **160** A553 – A558
[29] Kolosnitsyn V S, Kuzmina E V, Karaseva E V and Mochalov S E 2010 *J. Power Sources* **196** 1478–1482
[30] Zhang Z Y, Lai Y Q, Zhang Z A, Zhang K and Li J 2014 *Electrochim. Acta* **129** 55–61